UMERC+METS
2024 Conference

7-9 August | Duluth, MN, USA

Using Fiducial Markers for Pose Estimation of an OSWEC in a Wave Tank

Fanny Callisaya[1], Henry Yau[1], Krish Thiagarajan[1*], Mohamed A. Shabara[2]

[1]*Department of Mechanical & Industrial Engineering, University of Massachusetts Amherst, Amherst, MA, USA*
[2]*National Renewable Energy Laboratory, Golden CO, USA*

Abstract

In this study, we consider a novel method of sensing the motion of a wave energy converter in a wave tank under the influence of incoming waves. The wave energy converter considered in our research is an oscillating surge wave energy converter, which is a hinged paddle that responds to incoming waves. Motion sensing is normally done with inertial sensors, which can hinder motion due to suspended cables that carry power and transmit signals. Our proposed method is contactless and can be implemented economically. A camera is used to record different marker patterns affixed to the moving paddle and the motion deduced by pose estimation algorithms.

Fiducial markers are commonly used for robot localization and in augmented reality. There are many types of fiducial markers, including ArUco-type markers which are accurate, fast and robust. The system consists of markers attached to the paddle element and recorded using a machine vision camera. A pose estimation algorithm is then applied to the detected markers to estimate the tilt of the paddle. In this work, we examine the challenges of image acquisition and calibration for underwater targets, compare the motion obtained by this new system with a calibrated tilt sensor and identify areas where the new system may be superior.

Keywords: pose estimation; wave energy converter; computer vision; fiducial marker; wave tank experiments.

1. Introduction

The authors have been working on oscillating surge wave energy converters (OSWEC) by conducting design development, experimental studies and simulations. The Variable Geometry OSWEC (VGOSWEC) was developed with techno-economic performance in mind, as studies completed at NREL and other DOE national labs suggest that the most significant cost driver for WEC technologies is the structural design [1, 2]. The high structural costs are driven by the extreme waves that WEC structures must withstand; limiting and controlling those peak loads enables leaner and cheaper structures to be built. The annual energy production (AEP) has the greatest impact on LCOE in that it has a 1:1 relationship (i.e., a 10% increase in AEP results in a 10% reduction in LCOE). For this reason, the OSWEC remains promising because it has demonstrated through numerical and physical models that it can obtain the highest

* Corresponding author. krish.sharman@umass.edu

energy conversion efficiencies when compared with other WEC technologies [3]. NREL's VGOSWEC [4, 5], was granted a U.S. patent (Patent Number 10,066,595 B2) and revisions to the design including elevating above the seabed (Fig. 1) are currently studied [6]. As a precursor to the VGOSWEC, theoretical and experimental studies were completed on a bottom raised OSWEC [7 -9]. The boundary value problem was formulated as a potential flow past a thin bottom-hinged oscillating paddle in elliptical coordinates. Closed-form solutions for the added mass, radiation damping, and excitation forces/torques were obtained using angular Mathieu and Hankel-Mathieu functions. Corresponding experiments were conducted on a thin box shaped paddle (Fig. 2) where the motion was initiated by regular waves incident on the paddle, and the angular motion response measured by an inertial (tilt) sensor (also shown in Fig. 2).

Although the tilt sensor was calibrated and provided accurate measurements, some limitations were inevitable. The mass of the tilt sensor had to be included in the equilibrium calculation of the paddle. The sensor cables had to be connected to a retractable support to ensure that the former did not restrain the paddle motion. Given that the motion magnitudes are small to begin with, even small distractions can contribute to errors in measurement. It was thus desired to develop a non-contact system for laboratory use that is also economical to implement.

Figure 1: Artistic rendering of the VGOSWEC mounted on a raised foundation with PTOs shown in yellow.

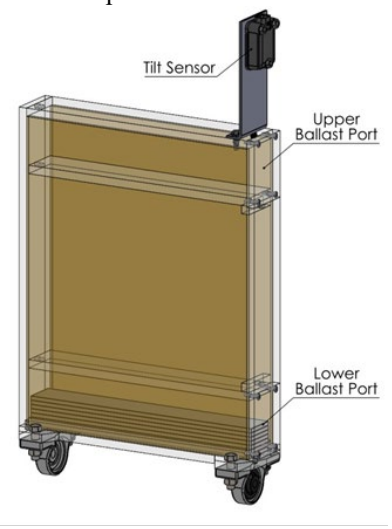

Figure 2. Artistic rendering of the VGOSWEC mounted on a raised foundation with PTOs shown in yellow. From [8, 9].

2. Methodology

2.1. Computer vision pose estimation

As the OSWEC model is constrained to a single degree of freedom, a simple computer vision pose estimator can be constructed using two detectable points on the model and a reference horizon. However, this method would also require a camera to be aligned precisely, with its sensor plane parallel with the model, or have its orientation relative to the model be known precisely. There are more robust methods that relax these requirements.

Perspective-n-Point (PnP) [10] is a classic computer vision problem with many well-developed algorithms to solve it. The goal of a PnP solver is to perform a 6DOF camera pose estimation using a set of known real-world positions that correspond to a set of points which can be identified in a 2D image captured by a camera. PnP is first used in the camera calibration step, where the intrinsic camera parameters are estimated, with a set of images taken of a checkerboard pattern in various poses. With the estimated camera intrinsics and by fixing the camera while moving a known target pattern, the 6DOF pose of the target can be estimated. The remaining task is choosing a target with uniquely identifiable points.

As a starting point, numerous circles assembled symmetrically could be trusted to estimate position of moving objects in a 3D world, whose points are then mapped into a 2D image. Circles are robust to noise, distance and blur. MATLAB has an in-built function called ***estworldpose*** for stochastic pose estimation, which can be used to measure the angular position of the paddle. The ***estworldpose*** function requires 3 inputs to do 3D pose estimation from 2D

image data. The camera intrinsic parameters matrix, the 3D world coordinates matrix and the output matrix of ***imfindcircles*** that contains the centers of detected circles. Good detection depends on image adjustment, otherwise false positives comprising of extra, fewer or no circles could occur.

We chose an arbitrarily large number of circular markers on the expectation that it could improve accuracy. Figure 3 shows a target composed of 140 markers symmetrically separated along 7 columns and 20 rows, The target was printed on a non-reflective-waterproof sheet of white paper and installed on the underwater model. The MATLAB function ***estworldpose*** ended up having very low repeatability when tested over 20 repetitions. Furthermore, pitch angles could not be detected correctly for all positions of the oscillating paddle due to not having a fixed initial point. It was observed that as the paddle moved from left to right, the initial point shifted from the top right corner to the top left. This inconsistency resulted in inaccurate measurements.

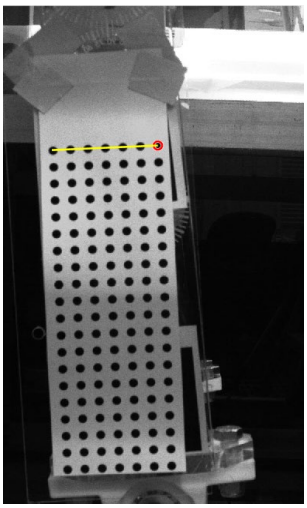

Figure 3. A pattern of circles affixed to a moving paddle and used as markers for pose estimation.

2.2. Fiducial markers for machine vision

Recently, binary-encoded fiducial patterns that can be identified by machine vision cameras have become popular. After a survey of common fiducial markers, we chose to use the OpenCV implementation of the ArUco [11] marker detection system as the next choice in our experiments. The ArUco marker, developed for augmented reality and robotics, is a popular choice due to its robustness to noise and motion. Each marker consists of a unique combination of white blocks in a black square surrounded with a white background. This pattern corresponds to a unique identifier which is defined in a standardized dictionary. An example marker is shown in Figure 4. When called, the detection function returns the identifier number and the image space coordinates of the four corners of any marker it detects. These corner points provide the inputs for the pose estimation algorithm.

Initial experiments using a solid paddle OSWEC model outside of the water tank indicated that a single marker was not sufficient to produce a good estimate of orientation. Therefore, two 67.5 mm square markers placed 326 mm apart were used. There are at least two methods to use with the individual markers. One method is to compute the pose of each marker separately and then use spherical linear interpolation to create an overall estimate of the orientation. Another is to use the eight corners directly in the PnP algorithm. The latter method was chosen as it appeared to provide greater robustness to errors in corner detection. For example, in Figure 5, the lower marker has a poor estimate of one corner and using the first method would create a poor estimated pose of the lower marker. Therefore, the second method was used in conjunction with a SQPnP solver [12]. The SQPnP solver casts the PnP problem as a quadric programming problem and solves for local minima with sequential programming with a guarantee that one of the local minima will be a global minimum.

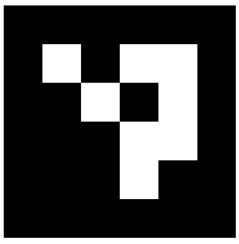

Figure 4. Sample ArUco fiducial marker.

3. Calibration tests for ArUco markers

A Microstrain MV5-AR tilt sensor mounted atop the OSWEC model (Fig. 2) was used to provide baseline measurement of the motions of the model. The MV5 is an IMU based orientation sensor that uses an Extended Kalman filter (EKF) to produce a measurement quantized in 0.1 deg steps. The measurements appear to be biased to minimize drift in the tilt and roll direction at the cost of having a clear drift in the yaw. The sample rate can be increased to a maximum of 500 Hz. An Allied Vision 1800 U-158C machine vision camera (maximum resolution of 1088×1456) with an Edmunds Optics 4mm/F1.8 lens was used to record videos. The exposure time was set to .012 ms which equates to a maximum of approximately 83 frames per second.

A series of tests were performed, consisting of the OSWEC mounted upside down in the tank without water including a decay test performed by allowing the OSWEC to swing freely. This setup is shown in Figure 5 along with an estimated coordinate triad and detected corners of each ArUco marker. A time history of the tilt sensor readings and the CV based estimate of pitch are shown in Figure 6 when the camera was placed 1 m away from the model, roughly parallel. Other camera incident angles were tested with similar results. The RMS difference between the MV5 sensor and the 8-point CV method was 0.54 degrees, which is an acceptable value considering the resolution of the MV5 is only 0.1 degrees. Despite a relatively short exposure time, there is some motion blur present in some images. Although ArUco markers are more robust to blur and noise than most other types of markers, there were instances where the lower marker was not detected. Shortening the exposure time meant increasing the illumination, which caused reflections on the glass tank degrading the image quality. However, as the OSWEC moves significantly slower when in water under only the influence of wave motion, there was confidence to move forward with the submerged OSWEC testing.

4. Experiments to measure OSWEC motion in waves

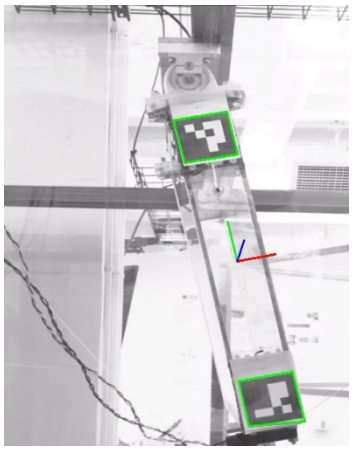

Figure 5. Setup used for decay tests conducted in the dry with model in pendular motion.

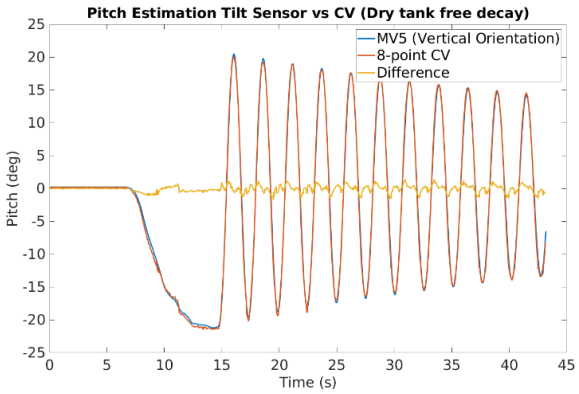

Figure 6. Pitch motion estimates from the tilt sensor (MV5) and the computer vision (CV) algorithm. Difference between the two measurements is in the order of 0.5 deg.

For the submerged test, the OSWEC model was supported on a pedestal, and allowed to oscillate about its hinge at the base (see Figs. 1 and 2) which altered the placements of the markers. A cross bar of the aluminum frame used to hold the VGOSWEC model also obstructed a complete view of the model. Therefore, the markers were placed closer together at 150 mm apart and the camera was moved closer to 30 cm away from the model (Fig. 7). A third marker was placed on the glass opposite the camera. This target was leveled using a bubble level and served as a reference horizon. These markers were created using a laser printer on waterproof paper and affixed using double sided tape. A sample frame is shown in Figure 8. The camera parameters were recomputed using a calibration board placed in the water and moved into various poses while the camera remained fixed. The wavemaker was run using a period of 2.8 s with a stroke of 66 mm (wave height of 53 mm) which produced a paddle pitch amplitude of approximately 6 degrees.

To reduce the noise, a constant acceleration motion model tracking Kalman filter was applied to the pose estimate results. The results are shown in Figure 8. The Kalman filter does well to remove outliers and results in an RMS difference of 0.39 deg. The improvement over the dry test can be attributed to the reduced speed reducing blur, reduced reflections due to the tank being filled, and the increased marker pixel coverage.

Additional tests for other wave conditions were also performed. Figure 10 shows one time history of the pitch motion with an amplitude of only 0.3 deg. The signal to noise ratio is much smaller at low motion amplitudes and the Kalman filter becomes necessary. As seen in the figure, the tilt sensor shows a mean drift, whereas the CV based method did not appear to have that bias.

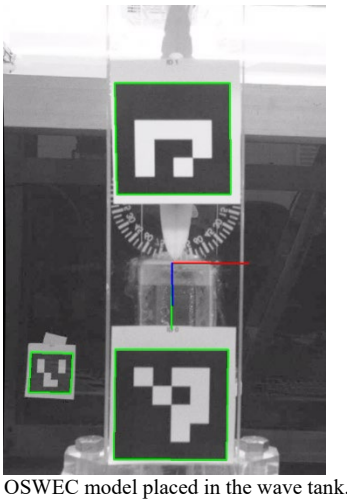

Figure 7. OSWEC model placed in the wave tank. ArUco markers were laminated and affixed to the model.

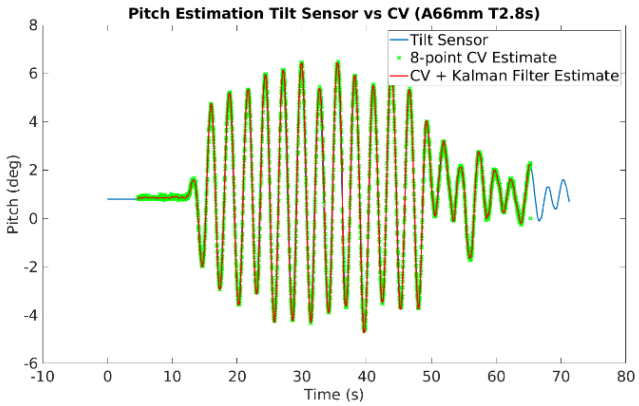

Figure 8. Pitch motion estimates from the tilt sensor (MV5) and the computer vision (CV) algorithm. Differences are barely visible.

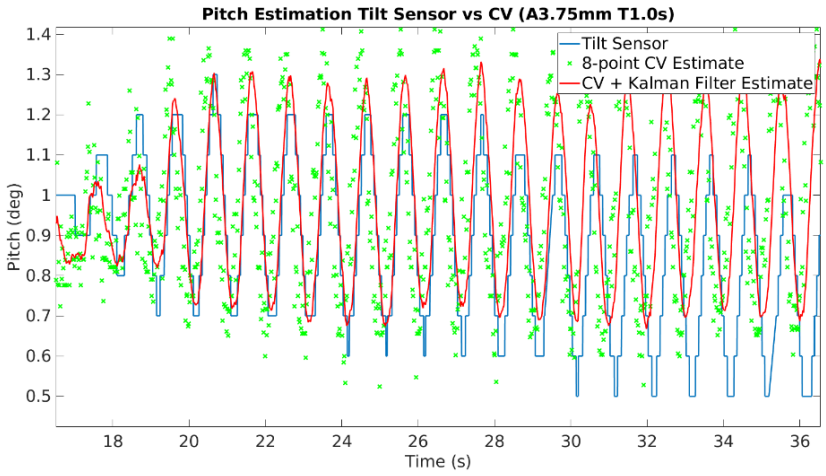

Figure 9. Pitch motion measurements at wave frequency of 1 Hz and amplitude of 3.75 mm. The pitch amplitude is less than half a degree. The tilt sensor appears to drift with time, while the CV measurements held steady.

5. Conclusions

There are situations where using a physical sensor such as the MV5 tilt sensor may hinder the quality of the recorded data. The additional mass and the cable management are both concerns for our VGOSWEC project. We demonstrated in this paper that computer-vision based pose estimation method can serve as a viable alternative to using physical sensors. The sample rate is only limited by the frame rate of the camera, as the video can be processed offline. While our MV5 tilt sensor can sample at up to 500 Hz or 2ms per time step, the computer vision approach is limited to 50 - 100 Hz.

Our experiments suggest that the pose algorithm estimates generally match well with the MV5 tilt sensor. The discrepancies at very low amplitudes may be due to inaccuracies in the MV5 which manifested as a drift. At low amplitudes, appropriate filtering becomes even more necessary as the signal to noise ratio decreases significantly.

Future developments planned include using higher resolution image sensors and high-speed cameras. With a precision rotary encoder mounted on the OSWEC shaft, we can accurately measure the angular displacement and calibrate the pose estimation accurately. The pose estimation algorithm could be improved further with a Kalman filter tracking algorithm that considers the constrained motion of the OSWEC devices. On the other hand, the CV approach could also be used in conjunction with an IMU to create a sensor fusion Kalman filter estimator that corrects for the IMU drift.

Acknowledgements

Work for this paper was conducted under the support of the US DOE Sapling Award to the National Renewable Energy Laboratory, and a sub-award to the University of Massachusetts Amherst. The authors are grateful to Dr. Nathan Tom for his pioneering work with the VGOSWEC, while as part of NREL. Prior work by Jacob Davis and Nhu Nguyen when at UMass Amherst are also acknowledged.

This work was authored in part by the National Renewable Energy Laboratory, operated by Alliance for Sustainable Energy, LLC, for the U.S. Department of Energy (DOE) under Contract No. DE-AC36-08GO28308. Funding provided by U.S. Department of Energy Office of Energy Efficiency and Renewable Energy Water Power Technologies Office. The views expressed in the article do not necessarily represent the views of the DOE or the U.S. Government. The U.S. Government retains and the publisher, by accepting the article for publication, acknowledges that the U.S. Government retains a nonexclusive, paid-up, irrevocable, worldwide license to publish or reproduce the published form of this work, or allow others to do so, for U.S. Government purposes.

References

[1] Neary, V. S., Mirko P., Jepsen, R. A., Lawson, M. J., Yu, Y-H., Copping, A., Fontaine, A. A., Hallett, K. C., and Murray. D. K. 2014. "Methodology for design and economic analysis of marine energy conversion (MEC) technologies." Albuquerque, NM: Sandia National Laboratories. SAND2014-9040.

[2] Jenne, D. S., Yu, Y.–H., and Neary. V. 2015. "Levelized Cost of Energy Analysis of Marine and Hydrokinetic Reference Models," Proceedings of the Water Power Week – 3rd Marine Energy Technology Symposium, April 27—29, 2015, Washington, D.C., United States.

[3] Babarit, A. 2015. "A Database of Capture Width Ratio of Wave Energy Converters." *Renewable Energy,* 80: 610–628.

[4] Tom, N. M., M. J. Lawson, Y.-H. Yu, and A. D. Wright. 2016. "Development of a Nearshore Oscillating Surge Wave Energy Converter with Variable Geometry." *Renewable Energy* 96: 410—424.

[5] Tom, N.M., Y.-H. Yu, A. D. Wright, and M. J. Lawson. 2017. "Pseudo-spectral control of a novel oscillating surge wave energy converter in regular waves for power optimization including load reduction." *Ocean Engineering* 137: 352—366.

[6] Burge, C., N. Tom, K. Thiagarajan, J. Davis, and N. Nguyen. 2021. "Performance modeling of a variable-geometry oscillating surge wave energy converter on a raised foundation," Proceedings of the 40th International Conference on Ocean, Offshore, and Arctic Engineering, June 25—30, Virtual Conference. https://www.nrel.gov/docs/fy21osti/78852.pdf

[7] Husain, S., J. Davis, N. Tom, K. Thiagarajan, C. Burge, and N. Nguyen. 2022. "Influence on structural loading of a wave energy converter by controlling variable-geometry components and the power take-off," Proceedings 41th International Conference on Ocean, Offshore, and Arctic Engineering, June 5—10, Hamburg, Germany. https://www.nrel.gov/docs/fy22osti/81883.pdf.

[8] Nguyen, N., J. Davis, K. Thiagarajan, N. Tom, C. Burge. 2021. "Optimizing power generation of a bottom-raised oscillating surge wave energy converter using a theoretical model," Proceedings of the 14th European Wave and Tidal Energy Conference, September 5—9, Plymouth, United Kingdom.

[9] Davis, J. 2021. Design and testing of a foundation raised oscillating surge wave energy converter. Master of Science Thesis. University of Massachusetts Amherst.

[10] Fischler, M. A. and R. C. Bolles. 1981. "Random sample consensus: a paradigm for model fitting with applications to image analysis and automated cartography". Commun. ACM 24, 6 (June 1981), 381–395. https://doi.org/10.1145/358669.358692

[11] S. Garrido-Jurado, R. Munoz-Salinas, F. J. Madrid-Cuevas, and M. J. Marin-Jimenez. 2014. "Automatic generation and detection of highly reliable fiducial markers under occlusion". Pattern Recogn. 47, 6 (June 2014), 2280-2292. DOI=10.1016/j.patcog.2014.01.005

[12] Terzakis, G. And M. Lourakis, 2010 "A Consistently Fast and Globally Optimal Solution to the Perspective-n-Point Problem". In A. Vedaldi, H. Bischof, T. Brox, & J.-M. Frahm (Eds.), *Computer Vision -- ECCV 2020* (pp. 478–494). Cham: Springer International Publishing.